


Targeted cyclooxygenase-2 inhibiting nanomedicine results in pain-relief and differential expression of the RNA transcriptome in the dorsal root ganglia of injured male rats

Andrea M Stevens^{1,2,3}, Muzamil Saleem^{1,2,3} , Brooke Deal^{1,2,3}, Jelena Janjic^{3,4}, and John A Pollock^{1,2,3} 

Molecular Pain
Volume 16: 1–19
© The Author(s) 2020
Article reuse guidelines:
sagepub.com/journals-permissions
DOI: 10.1177/1744806920943309
journals.sagepub.com/home/mpx


Abstract

Chronic constriction injury of the sciatic nerve in rats causes peripheral neuropathy leading to pain-like behaviors commonly seen in humans. Neuropathy is a leading cause of neuropathic pain, which involves a complex cellular and molecular response in the peripheral nervous system with interactions between neurons, glia, and infiltrating immune cells. In this study, we utilize a nonsteroidal anti-inflammatory drug -loaded nanoemulsion to deliver the cyclooxygenase-2 inhibitor, Celecoxib, directly to circulating monocytes following nerve injury, which provides long-lasting pain relief. However, it is not fully understood how cyclooxygenase-2 inhibition in a macrophage traveling to the site of injury impacts gene expression in the dorsal root ganglia. To elucidate aspects of the molecular mechanisms underlying pain-like behavior in chronic constriction injury, as well as subsequent pain relief with treatment, we employ RNAseq transcriptome profiling of the dorsal root ganglia associated with the injured sciatic nerve in rats. Using high throughput RNA sequencing in this way provides insight into the molecular mechanisms involved in this neuroinflammatory response. We compare the transcriptome from the dorsal root ganglia of the following study groups: chronic constriction injury animals administered with cyclooxygenase-2 inhibiting celecoxib-loaded nanoemulsion, chronic constriction injury animals administered with vehicle treatment, a drug-free nanoemulsion, and a group of naïve, unoperated and untreated rats. The results show an extensive differential expression of 115 genes. Using the protein annotation through evolutionary relationship classification system, we have revealed pain-related signaling pathways and underlying biological mechanisms involved in the neuroinflammatory response. Quantitative polymerase chain reaction validation confirms expression changes for several genes. This study shows that by directly inhibiting cyclooxygenase-2 activity in infiltrating macrophages at the injured sciatic nerve, there is an associated change in the transcriptome in the cell bodies of the dorsal root ganglia.

Keywords

Neuropathic pain, chronic constriction injury, neuroinflammation, celecoxib, nanoemulsion, RNA sequencing

Date received: 5 April 2020; revised: 18 May 2020; accepted: 1 June 2020

Introduction

Peripheral neuropathy is characterized as damage or injury to the peripheral nervous system resulting in spontaneous pain, allodynia, and mechanical and thermal hyperalgesia. A key mechanism underlying peripheral neuropathy is neuroinflammation, which is thought to be more efficient at driving chronic pain than systemic inflammation,¹ as it involves the induction of the innate

¹Bayer School of Natural and Environmental Sciences, Duquesne University, Pittsburgh, PA, USA

²Department of Biological Sciences, Duquesne University, Pittsburgh, PA, USA

³Chronic Pain Research Consortium, Duquesne University, Pittsburgh, PA, USA

⁴Graduate School of Pharmaceutical Sciences, Duquesne University, Pittsburgh, PA, USA

Corresponding Author:

John A Pollock, Duquesne University, 600 Forbes Avenue, Pittsburgh, PA 15282, USA.

Email: pollock@duq.edu



immune response as well as activation of the nervous system. Interactions between injured neurons, glia, and infiltrating immune cells result in the production of effector molecules known as inflammatory mediators, all of which contribute to the hypersensitive state. It is previously known that the release of inflammatory mediators contributes to the induction and maintenance of neuropathic pain leading to the alteration of neuronal function both at the site of injury as well as at the site of neuronal cell bodies in the dorsal root ganglia (DRG).^{2–5} Sensitization of the injured nerve and its associated neuronal cell bodies in the DRG may lead to long-term changes in gene expression in these cells, as suggested by RNA transcriptome studies.^{6–8}

We have utilized a neuropathic pain model in male rats known as chronic constriction injury (CCI) of the sciatic nerve.^{4,5,9–15} Within hours of CCI, activation of the inflammatory response occurs, resulting in cellular and molecular expression changes at and near the site of injury.^{4,16} The production of inflammatory mediators along with the activation of immune-like glial and immune cells leads to shifts in cellular phenotypes, which further results in changes in gene expression that signals hypersensitivity and chronic pain in CCI animals.^{16–19} We have previously reported on gene expression changes that occur at the site of injury at the sciatic nerve for messenger RNAs (mRNAs) involved in neuroinflammation as well as in the associated DRG.^{15,20} For example, we have previously shown that CCI-associated hypersensitivity is associated with GAP43, NPY, and TRPV1 mRNA expression changes in the DRG and furthermore, that TRPV1 protein expression changes in specific CCI DRG cell bodies of neurons that innervate the affected foot (identified by DiD retrograde labeling).²⁰ In other studies, quantitative polymerase chain reaction (qPCR) of mRNA expression in the injured sciatic nerve for 84 neuroinflammatory genes revealed several distinct differences between naïve, CCI, and CCI treated with cyclooxygenase-2 (COX-2) inhibition.¹⁵ Changes in the expression of mRNAs for cytokines and chemokines is consistent with the inflammation and corresponding infiltration of macrophages at the site of injury. Furthermore, the expression of transcripts for integrins involved with selective macrophage adhesion as well as changes in neuronal and glia expression profiles were observed in the sciatic nerve dependent on the pain or pain-relieved state.¹⁵ Administration of a macrophage-targeted COX-2 inhibiting celecoxib-loaded nanoemulsion (CXB-NE) revealed that by targeting the production of PGE₂ at the site of injury, pain relief is associated with a partial reversal of the gene expression profiles in the sciatic nerve when compared to tissue in a pain state.¹⁵ Here, we hypothesize that ultimately, the inflammatory milieu and tissue response at the site of injury are communicated to the DRG where

changes in expression profiles are of particular importance given that these cells are a component of primary sensory neurons, acting as the bridge between the peripheral and central nervous system.

RNA sequencing allows for the exploration of the molecular and biological mechanisms of neuropathic pain through the analyses of whole transcriptome changes after nerve injury. Using RNA sequencing, several studies have previously examined pain-associated changes in expressed RNA in the DRG.^{8,21–24} Here, we report studying changes in the RNA transcriptome in the DRG when the CCI animal is experiencing significant pain as compared to a naïve animal and separately for animals that are treated with an anti-inflammatory nanoemulsion (COX-2 inhibiting CXB-NE). The nanoemulsion pain-relieving therapy selectively targets the COX-2 in macrophages, which is normally produced by these infiltrating cells and other activated cells at the site of injury, triggering pain.²⁵ The nonsteroidal anti-inflammatory drug (NSAID) CXB can be used to treat pain through the reduction of PGE₂ following selective inhibition of COX-2. We have previously shown that localized delivery of a single micro-dose (0.24 mg/kg) of CXB in nanoemulsion, which is incorporated in circulating macrophages/monocytes that then naturally accumulate at the site of injury provides up to six days of pain relief.^{5,14,15,25} An important feature is that the nanomedicine delivers drug to the affected injured nerve.^{5,14,15} This creates a unique opportunity to assess drug effects on cellular expression of RNAs when the drug is present at the distal injury and virtually no other parts of the peripheral nervous system. With this approach, we have been able to reveal transcriptome changes in the DRG associated with CXB-NE. Results show that DRG RNAs in CCI-treated males exhibit differential expression in association with changes in neurons, activated glial cells, and multiple immune cells.

Materials and methods

Animals

Adult male Sprague–Dawley rats (Hilltop Animals, Springdale, PA) weighing 200 to 225 g at the time of surgery were treated in accordance with the guidelines outlined in the Guide for the Care and Use of Laboratory Animals of the National Institutes of Health and Duquesne University's approved protocol (no. 1501–01 and no. 1803–02) by the Institutional Animal Care and Use Committee. Efforts were made to minimize the number of animals used in this study and the time experiencing pain. Animals were acclimated for five days to standard living conditions, kept on a 12-hour light, 12-hour dark cycle, and given food and water *ad libitum*. Animals were kept on paper bedding

and socially housed until the time of surgery after which they were then individually housed. All animals were fed a special diet to avoid autofluorescence during imaging (Research Diets, Inc., New Brunswick, NJ; catalog no. AIN-93G).

CCI-induced neuropathic pain

Peripheral nerve injury was induced (this was designated “day 0”) using CCI as first described by Bennett and Xie⁹ and adapted previously.^{4,5,14,15} Briefly, CCI causes inflammation and subsequent pain when chronic gut sutures are loosely tied around the common sciatic nerve in the animal’s hindleg. Animals are anesthetized with inhaled isoflurane and oxygen. Surgery is performed with a heat lamp and heating pad to ensure maintenance of body temperature and vital signs are monitored throughout via tail flick. Aseptic technique was used for all surgical procedures. A superficial incision in the skin, 3 to 4 mm below the femur is done, followed by a cut through the connective tissue between the underlying biceps femoris and gluteus superficialis muscles to expose the sciatic nerve. An approximate 8 mm section of the sciatic nerve was isolated and four sutures (McKesson 4-0 Chromic Gut, catalog no. S653GX) were placed 1 mm apart on the common sciatic nerve to ligate it. Naïve, unoperated rats were used as a control. For RNA sequencing, naïve rats ($n=3$), CCI rats given drug-free nanoemulsion (CCI DF-NE; $n=4$), and CCI rats given CXB-NE (CCI CXB-NE; $n=3$) were compared.

Behavioral testing

Mechanical allodynia testing of both hind-paws was conducted using von Frey monofilaments of increasing diameters using the up-down method as described previously.^{5,14,15,26} Behavioral testing was conducted twice before surgery (day 0), and days 2 through 12 after surgery, with a rest day on the day of and after surgery. The 50% paw withdrawal threshold was calculated and treatment groups were analyzed by two-way analysis of variance (ANOVA) and post hoc Tukey testing using GraphPad Prism 8.0.^{5,15}

Nanoemulsion administration

CXB-NE and drug-free nanoemulsion (DF-NE) (vehicle)^{5,14,15,25,27} treatments were randomized and blinded to investigators. Nanoemulsion was administered on day 8 when the animal is reaching a plateau of pain behavior.^{4,14,15} Animals were lightly anesthetized and administered nanoemulsion through intravenous tail vein injection as previously described.²⁸ After nanoemulsion enters the bloodstream, it is picked up by circulating macrophages/monocytes through phagocytosis; the

macrophages naturally accumulate at the site of injury.^{5,14,27,29}

Tissue dissection and RNA extraction

On day 12, a total of 10 animals (3 Naïve, 4 CCI DF-NE, and 3 CCI CXB-NE) were euthanized via humane carbon dioxide inhalation. Ipsilateral L4 and L5 DRGs were immediately collected and stored in RNAlater (Life Technologies, New York, NY) for 24 hours at room temperature and then kept at -20°C until RNA extraction. Ipsilateral DRGs from L4 and L5 for each individual animal were combined and used for RNA extraction. Total DRG RNA was isolated with a Qiagen RNeasy Plus Mini Kit (Qiagen Inc, Valencia, CA) according to manufacturer’s instructions. Quality was initially checked using the NanoDrop 1000 (Thermo Fisher Scientific, Waltham, MA). RNA quantification was performed using a Qubit (Thermo Fisher Scientific) and integrity was measured with Tape Station (Agilent, Santa Clara, CA). Only RNA samples with a minimum RNA integrity number value above 6.6 were used for sequencing.³⁰

Whole transcriptome RNA sequencing

Total RNA was analyzed using an Illumina sequencer for each condition. Library preparation was performed according to manufacturer’s instructions using the Takara SMARTer Stranded Total RNA-Seq Kit, Pico input Mammalian v1 (Mountain View, CA), with 2 ng total RNA input. Total RNA is converted to complementary DNA (cDNA) via reverse transcription with random hexamers and proprietary code-switching technology, which maintained RNA strand information. Five cycles of PCR added barcode sequencing indexes followed by double SPRI size selection. Ribosomal cDNA was depleted via the cleavage with Zap-R and mammalian-specific R-probes. Remaining library was enriched with 12 cycles PCR followed by SPRI bead reaction clean up. Library was loaded on a NextSeq500 (Illumina, Hayward, CA) at 1.8 pM with 20% Phi-X. The sequences were trimmed and reads with a minimum of 75 base pairs were used. RNA sequencing was performed by the Genomics Research Core at the University of Pittsburgh.

Differential expression analysis

The resulting sequencing data were mapped to the *Rattus norvegicus* reference genome from ENSEMBL using HISAT whole genome and SALMON whole transcriptome mapping. Reads per kilobase per million mapped reads were calculated for each gene hit count to determine the expression levels. Relative differential expression analysis for each transcript between the

groups was calculated as the number of readings mapping to each transcript normalized by the transcript length and the total number of mapped reads using Student's *t* test. Differential expression analysis was done in conjunction with the Genomics Analysis Core at the University of Pittsburgh. Raw P values and adjusted P values (false discovery rate; FDR values) were calculated for all genes. We report data as significant if the raw P value ≤ 0.05 and/or the FDR value ≤ 0.50 to ≤ 0.05 . The statistical measurement used is indicated within each given dataset. Heatmaps were generated using Prism 8 Version 8.4.2. Genes with expressed RNAs shared between all three conditions (Naïve, CXB-NE, and DF-NE) and that had an FDR ≤ 0.05 were selected resulting in the collection of 57. Values mapped were the Log_2 of the counts per million.

GO and enrichment analysis

Genes previously annotated based on relevant functional gene ontology (GO) descriptions were compared to our dataset using GO database.³¹ GO annotations and functional enrichment analysis were applied to investigate the roles of all differentially expressed genes between CCI DF-NE and CCI CXB-NE animals. Protein annotation through evolutionary relationship (PANTHER) pathway analysis based on functional classifications and GO analysis hierarchical categories according to the Biological Process, Molecular Function, and Cellular Components of the differentially expressed RNAs (<http://www.pantherdb.org>) of FDR ≤ 0.50 were used in Table 6 and Supplemental data (Supplemental Table 7). Kyoto Encyclopedia of Genes and Genomes (KEGG) Pathway functional analysis was performed using g:Profiler (version e99_eg46_p14_f929183) with a g:SCS multiple testing correction method applying a significance threshold of 0.05.³² Reactome pathway analyses³³ were also applied (FDR ≤ 0.05 ; <http://www.reactome.org>) to elucidate annotated pathways involved in the pain state when CXB-NE is administered compared to DF-NE to the pain state. All differentially expressed genes were applied to the Gene Expression Database³⁴ (<http://informatics.jax.org>) to further demonstrate their individual roles in the maintenance and transduction of neuropathic pain under CCI conditions when COX-2 is attenuated with CXB-NE.

Literature search of neuroinflammatory genes

A comprehensive literature search containing the search terms CCI, CXB, and each term category listed in Tables 7 and 8 was conducted in peer-reviewed primary literature databases (PubMed, Science Direct, PubMed Central, among others). In addition, the Gene

Expression Database³⁴ and GO PANTHER database were both utilized to help identify gene function.

Validation of genes by quantitative real-time PCR

The extracted total RNA from the DRGs was reverse transcribed into cDNA using RT² First Strand Kit (Qiagen, Germantown, MD) according to the manufacturer's instructions. qPCR using pooled L4 and L5 DRG tissues from rats from the RNA sequencing study and additional rats were used. qPCR was performed using individual RT² primer assays (Qiagen) on the ABI StepOnePlus cycler (Applied Biosystems, Waltham, MA) with RT² SYBR green with ROX (Qiagen) according to manufacturer's instructions. Each reaction was performed in triplicate and normalized to the housekeeping gene glyceraldehyde 3-phosphate dehydrogenase. Analysis was done using the Livak method³⁵ where fold change values were calculated compared to the naïve control group. A two-tailed Student's *t* test, standard deviation, and error were calculated. A one-way ANOVA followed by post hoc testing and Tukey's multiple comparison test with GraphPad Prism (version 8, San Diego, CA). A P value ≤ 0.05 was considered statistically significant in all analyses.

Results

Mechanical allodynia in CCI rats and relief from hypersensitivity with a microdose of CXB nanoemulsion

Consistent with previous studies, male rats experiencing sciatic nerve CCI^{4,9,14,15} exhibit peripheral neuropathy in the ipsilateral hindpaw, which can be demonstrated with footpad stimulation by von Frey monofilaments of increasing diameter. Behavioral testing of animals in this specific study illustrates a behavioral baseline (before animals receive surgery) of no significant difference in pain-like behavior among the populations in this study (Figure 1). Mechanical allodynia testing was not conducted on the day of surgery (day 0) but was continued on days 2 to 12 following CCI surgery. All CCI animals used in this study exhibit behavior indicative of increasing hypersensitivity up to day 8 (Figure 1), at which time the population was divided into naïve (no surgery and no injection treatment), those that receive intravenous injection of CXB-NE and those that receive an intravenous injection of DF-NE (vehicle). By day 10 (two days postinjection), animals receiving CXB-NE experience a statistically significant decrease in allodynia compared to those receiving vehicle (DF-NE; Figure 1). There is no statistically significant difference between CCI CXB-NE behavior and naïve rats on days 11 and 12 indicating that the CCI animals were experiencing

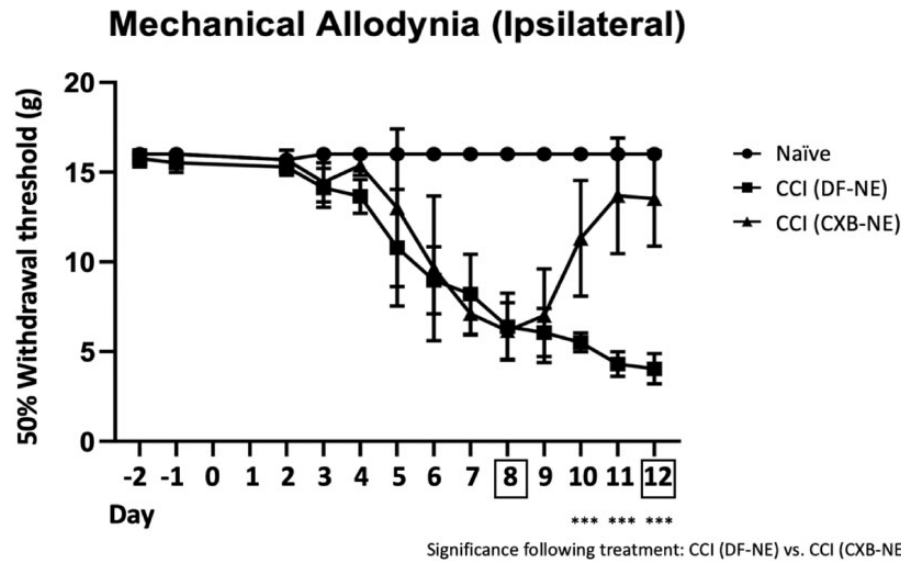


Figure 1. Pain relief behavioral testing of the animals used in this study and timeline of events following treatment. Celecoxib-loaded nanoemulsion (CXB-NE) reduces pain-like behavior in CCI animals within one day of administration compared to those receiving drug-free nanoemulsion as a vehicle (DF-NE). By day 12, injured rats given CXB-NE return to baseline behavior, whereas rats treated with CCI DF-NE continue to exhibit hypersensitivity (displayed as ***). Data are expressed as a mean \pm SD. Significance was determined by two-way ANOVA and post hoc Tukey's multiple comparison test ($P < 0.0001$). Animals underwent mechanical allodynia on the ipsilateral hindpaw two days prior to surgery (days -2 and -1), a rest day on day 0 (day of CCI surgery) and day 1, and continued von Frey testing until euthanasia (day 12). Tail vein injection of nanoemulsion occurred as pain-like behavior plateaus on day 8. All animals were euthanized on day 12.

significant pain relief, whereas the CCI DF-NE animals continue to reflect significant hypersensitivity (Figure 1).

RNAseq analysis

To identify transcriptional profiles of RNA in DRG experiencing peripheral nerve injury, high-throughput RNA sequencing was performed on total RNA extracted from DRG recovered from animals on day 12 post CCI surgery. Male rats were administered a single dose of nanoemulsion (0.24 mg/kg) intravenously on day 8 postsurgery, a time when pain-like behavior approaches a maximum. Total RNA was isolated from L4 and L5 ipsilateral DRG (and combined) for uninjured naïve rats as well as injured CCI (DF-NE) and CCI CXB-NE drug-treated rats. With alignment to the *Rattus norvegicus* reference genome, overall, the RNA sequencing of the naïve animal DRG produced 18.8 million raw sequences of which 12.7 million sequences mapped to the reference genome representing 21,152 transcripts from 14,717 genes (Table 1). The sequencing from CCI DF-NE animals represented 20.2 million raw sequences, 13.4 million mapped to the genome corresponding to 21,218 transcripts for 14,753 genes (Table 1). The analysis of the RNA from CCI CXB-NE DRG found 26.1 million raw

sequences, 18.8 million of which mapped to the rat genome, corresponding to 22,541 transcripts for 15,642 genes (Table 1).

The analysis shows that between 30% and 40% of the RNAs detected correspond to exonic elements that code for mRNAs that can be translated into protein (Figure 2). Noncoding base pairs comprising intronic and intergenic elements consist of the majority of the represented sequence elements that were detected. Intronic elements were expressed evenly in naïve and CCI DF-NE at 14%. A higher number of intronic sequences were detected for CCI CXB-NE at 21% overall (Figure 2). Intergenic elements dominated the detected RNAs; naïve 48%, CCI DF-NE 49%, and CCI CXB-NE 40% (Figure 2).

A comparison between RNAs detected in DRGs from vehicle (DF-NE), versus COX-2 inhibited (CXB-NE), and naïve shows that 8,948 distinct genes are expressed in all three conditions. Gene biotype analysis was performed for those RNAs that were differentially expressed showing that the majority of transcriptional changes were observed in protein-coding genes (94%). The remaining differentially expressed RNAs are considered noncoding, being composed of 111 (1.2%) RNAs of known long noncoding genes (lncRNAs) and as

Table 1. Mean number of raw and mapped reads, transcripts and genes detected, and standard deviation.

Condition	Naïve Control	CCI DF-NE	CCI CXB-NE
Raw sequences	$18.8 \times 10^6 \pm 1.2 \times 10^6$	$20.2 \times 10^6 \pm 2.9 \times 10^6$	$26.1 \times 10^6 \pm 1.1 \times 10^6$
Mapped sequences	$12.7 \times 10^6 \pm 8.4 \times 10^5$	$13.4 \times 10^6 \pm 2.2 \times 10^6$	$18.8 \times 10^6 \pm 8.1 \times 10^5$
Transcripts detected	21,152 ± 114	21,218 ± 524	22,541 ± 167
Genes detected	14,717 ± 90	14,753 ± 375	15,642 ± 118

Note: Mapped pairs are the total number of pairs for which both ends map; Transcripts/Genes Detected is the number of transcripts/genes with at least five reads. CCI: chronic constriction injury; CXB-NE: celecoxib-loaded nanoemulsion; DF-NE: drug-free nanoemulsion; M: Millions.

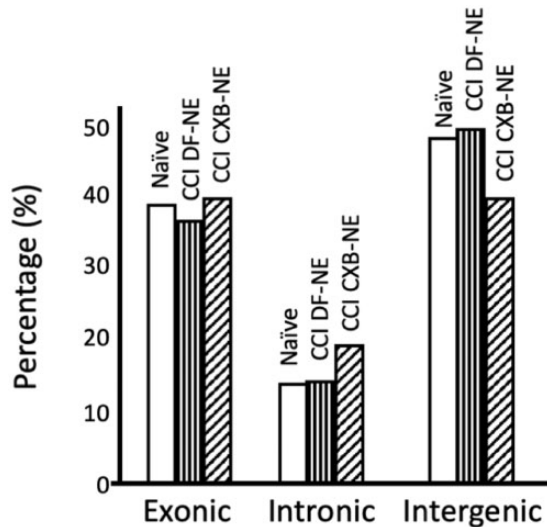


Figure 2. Distribution of gene elements. The mapped percentage of expressed exonic, intronic, and intergenic elements in naïve, CCI DF-NE, and CCI CXB-NE conditions. There is a higher percentage of intronic reads in CCI CXB-NE compared to naïve and CCI DF-NE and a lower percentage of intergenic reads. CCI: chronic constriction injury; DF-NE: drug-free nanoemulsion; CXB-NE: celecoxib-loaded nanoemulsion.

microRNAs (miRNAs; 0.07%). An additional 322 RNAs account for the remaining (2.79%) found within the samples but are not shown.

CCI of the sciatic nerve leads to differential expression of RNAs in the DRG

Table 2 shows the number of differentially expressed RNAs out of the 8,948 RNAs that were analyzed for statistically significant differences in the comparisons of control animals (naïve) versus CCI DF-NE (DF-NE) treated rats, control versus drug-loaded nanoemulsion (CXB-NE) treated CCI rats, and between the treated and untreated pain states. A comprehensive table of all statistical values studied is in Table 2, including the traditional “raw P values” of ≤ 0.05 and ≤ 0.001 and the more stringent False Discovery Rate (“FDR”) value ranging between ≤ 0.05 and 0.50. The FDR value

is the adjusted P value, and its interpretation is that with a raw P value of ≤ 0.05 , 5% of 100 of those are false positives. Although the traditional raw P values can still be reliably utilized, with the FDR, we can say with confidence that these values are not false positives. When compared to naïve-unoperated controls (pain free), CCI DF-NE (in pain) exhibited 183 total RNAs that were differentially expressed (raw P value ≤ 0.05) and 16 with a raw P value ≤ 0.001 . When the analysis calculates the adjusted P value (FDR ≤ 0.05) zero genes were revealed as significant; however, when the FDR value is increased to ≤ 0.50 and a raw P value ≤ 0.001 , 16 genes are differentially expressed; 9 up-regulated and 7 down-regulated. Interestingly, these are the same genes within both statistical categorizations. When comparing naïve (unoperated, pain free) to CCI CXB-NE animals, 584 total RNAs are differentially expressed with a statistically significant raw P value < 0.05 and 78 RNAs with a statistically significant FDR value (≤ 0.05). When comparing untreated injured animals, CCI DF-NE (pain) to CCI CXB-NE (COX-2 inhibiting nanoemulsion treated pain relieved) 675 genes differentially expressed were shown to be statistically significant (raw P value < 0.05). Of those RNAs, 487 were up-regulated in the pain relieved state (CCI CXB-NE), while 188 were down-regulated (in CCI CXB-NE; Table 2). When considering the adjusted P value (FDR) ≤ 0.05 for the comparison of CCI DF-NE (pain) to CCI CXB-NE (COX-2 inhibiting nanoemulsion treated pain relieved) 115 genes were found to be differentially expressed (Table 2). Of those 115 genes, 98 were up-regulated in pain relief (CCI CXB-NE) and 17 were down-regulated (in CCI CXB-NE; Table 2). All further differential expression analyses in this work focus on transcriptional differences among the pain state animals; all other data can be found in the Supplemental data (Supplemental Tables 1–6) section. Additionally, data reported in the Supplement includes all data with a significant P value (≤ 0.05).

Comparison of detected RNAs from CCI DF-NE (pain) to CCI CXB-NE (pain-relieved COX-2 inhibited) revealed significant changes in a total of 115 genes, 91 of which are considered protein-coding genes, 82 exhibiting

Table 2. Numbers of RNAs differentially expressed utilizing multiple statistical values.

	Naïve vs. CCI DF-NE	Naïve vs. CCI CXB-NE	CCI DF-NE vs. CCI CXB-NE
Raw P value data			
Differentially expressed ($P \leq 0.05$)	183	584	675
Upregulated genes	110	514	487
Downregulated genes	73	70	188
FDR data			
Differentially expressed ($FDR \leq 0.05$)	0	78	115
Upregulated genes	0	72	98
Downregulated genes	0	6	17
FDR data			
Differentially expressed ($FDR \leq 0.10$)	0	107	164
Upregulated genes	0	97	141
Downregulated genes	0	10	23
FDR data			
Differentially expressed ($FDR \leq 0.50$)	16	316	550
Upregulated genes	9	287	487
Downregulated genes	7	29	63
Raw P value data			
Differentially expressed ($P \leq 0.001$)	16	97	136
Upregulated genes	9	88	116
Downregulated genes	7	9	20

Note: Up-regulated and down-regulated values represent the latter condition compared (CCI DF-NE genes up- and down-regulated when compared to naïve, CCI CXB-NE genes up- and down-regulated when compared to naïve; and RNAs of CCI CXB-NE up- and down-regulated when compared to CCI DF-NE). CCI: chronic constriction injury; CXB-NE: celecoxib-loaded nanoemulsion; DF-NE: drug-free nanoemulsion; FDR: false discovery rate.

elevated expression while pain is relieved, with 9 genes down-regulated, and 24 representing noncoding transcripts; 57 of these genes are also shared with the naïve condition and their comparative expression levels visualized in Figure 3.

Table 3 illustrates the detailed information of the 25 up-regulated protein-coding genes with the greatest fold-change in expression along with their associated molecular function (NCBI database). During COX-2 inhibition (CCI CXB-NE), Prosaposin-like 1 (Psalp1) shows the highest expression change of 42-fold (essentially going from undetectable to expressed at a high level), with other notable genes including Leucine-rich repeat transmembrane neuronal 1 (LRRTM1), transient receptor potential cation channel, subfamily V3 (TrpV3), and potassium voltage-gated channel subfamily J, member 9 (Kcnj9) exhibiting an increased expression after administration of the anti-inflammatory CXB-NE (Figure 3). Table 4 illustrates those significant down-regulated protein-coding genes in CCI CXB-NE, having a raw P value <0.05 , with their protein function as reported by NCBI. Of the 17 down-regulated transcripts ($FDR \leq 0.05$) in the pain relief state (CCI CXB-NE) compared to the pain-state (CCI DF-NE), 9 of which are protein-coding (Table 4).

Of these differentially expressed genes in pain-state versus pain-relieved animals, four are previously

annotated lncRNAs, all of which experience an increased expression after CXB-NE (Table 5). While these lncRNAs are annotated in ENSEMBL, there is however no known role ascribed to their pathogenesis in neuropathic pain.

Functional enrichment analysis

To further examine the mechanisms of differentially expressed RNAs within the pain states, GO (<http://www.pantherdb.org>) annotation and functional enrichment analyses were performed.³¹ GO relies on grouping known genes into categories of common function. The number of genes within each GO category encompasses all genes reported with significant enrichment ($FDR \leq 0.05$) and that represent functional pathways already annotated (Table 6). This analysis shows that mRNAs exhibiting differential expression in this analysis are members of 14 functional pathways. We find there are up to 10 differentially expressed mRNAs in CCI DF-NE versus CCI CXB-NE that are evident in these 14 distinct pathways (Table 6 and Supplemental Table 7). GO revealed the most significantly enriched “biological processes” were the collection of “gene expression” (classified per its GO class as GO:0010467) and response to drug (GO:0042493; Supplemental Table 7). The most significantly enriched “molecular functions” include molecular

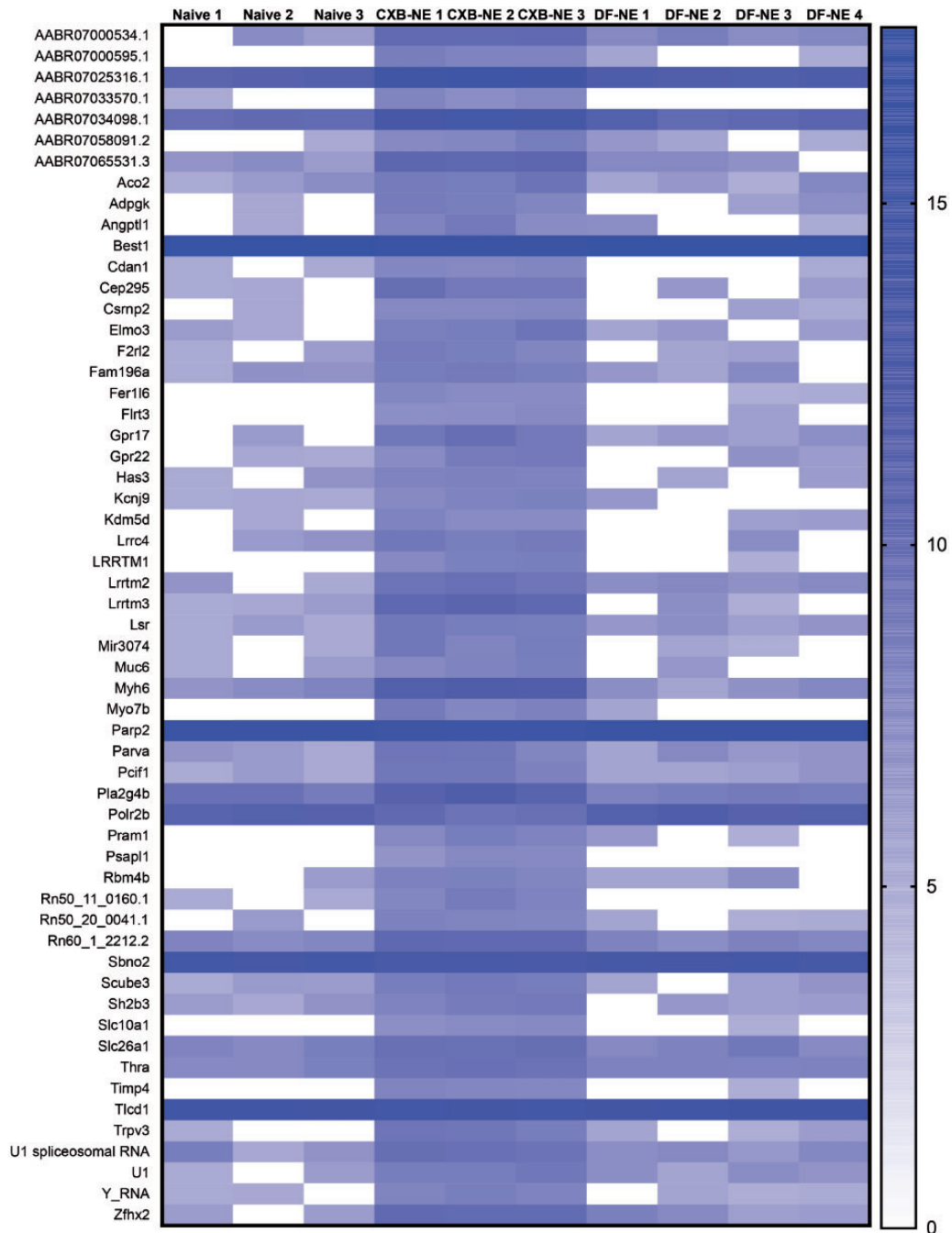


Figure 3. Heatmap showing \log_2 count per million (CPM) of the 57 genes shared across all 3 conditions with an adjusted P value (FDR) ≤ 0.05 .

transducer activity (GO:0060089) and signaling receptor activity (GO:0038023; Supplemental Table 7). The more specific, GO Slim analysis of molecular function reveals G-protein-coupled receptor activity (GO:0004930) and transmembrane signaling receptor activity (GO:0004888), both of which are noted in GO molecular function as well. Twenty statistically enriched cellular components are shown in the pain state when CXB-

NE and DF-NE animals are compared. Notable cellular components include membrane-bounded organelle (GO:0043227), intracellular membrane-bounded organelle (GO:0043231), and cytoplasmic part (GO:0044444; Supplemental Table 7).

KEGG signaling pathway analysis comparing 675 differentially expressed genes (raw P value ≤ 0.05) among CCI DF-NE and CCI CXB-NE conditions

Table 3. Top 25 up-regulated protein-coding genes differentially expressed between CCI DF-NE and CCI CXB-NE rats with an FDR <0.05.

Gene description	Gene ID	Fold change	FDR	ENSEMBL Gene ID	Molecular function
Prosaposin-like 1	Psalp1	42.204	0.00073	ENSRNOG00000006845	Neurotrophin/Growth Factor
Anterior gradient 2	Agr2	33.680	0.03118	ENSRNOG00000005023	Adhesion
Anti-silencing function 1A histone chaperone	Asf1a	33.637	0.00734	ENSRNOG00000000415	Histone chaperone
Leucine-rich repeat transmembrane neuronal 3	Lrrtm3	32.088	2.55E-24	ENSRNOG00000026466	Synaptic transmission
Nudix hydrolase 16 like 1	Nudt16l1	29.052	0.04646	ENSRNOG00000003224	Signal transduction
Membrane associated ring-CH-type finger 10	March10	27.061	0.04993	ENSRNOG00000007084	Ubiquitination
Myosin VIIb	Myo7b	23.855	3.40E-05	ENSRNOG00000015035	Adhesion
Myosin heavy chain 6	Myh6	22.701	4.00E-31	ENSRNOG00000025757	Adhesion
Transmembrane BAX inhibitor motif containing 1	Tmbim1	21.271	0.00016	ENSRNOG00000014797	Innate immune system
Leucine-rich repeat transmembrane neuronal 1	LRRTM1	21.265	0.00011	ENSRNOG00000006093	Synaptic transmission
Arrestin 3	Arr3	17.859	0.00384	ENSRNOG00000002904	Signal transduction
Tissue inhibitor of metalloproteinase 4	Timp4	16.811	8.52E-05	ENSRNOG00000007955	Signal transduction
Codanin 1	Cdan1	16.177	0.00083	ENSRNOG00000047427	Cytoskeletal
Centrosomal protein 295	Cep295	14.559	3.40E-07	ENSRNOG00000010999	Centriole biosynthesis
Similar to Vomeromodulin	LOC690507	13.594	0.02271	ENSRNOG00000015637	Signal peptide for olfaction
Fanconi anemia, complementation group AABR07000595.1	Fancc	12.978	0.00461	ENSRNOG00000016889	Complement
MYC binding protein 2, E3 ubiquitin protein ligase	AABR07000595.1	12.822	0.00014	ENSRNOG00000030796	Unknown
Solute carrier family 10 member 1	Mycbp2	12.429	0.0155	ENSRNOG00000010479	Axon guidance and Signal transduction
Leucine zipper protein 1	Slc10a1	12.363	0.0043	ENSRNOG00000005794	Ion channel
Transient receptor potential cation channel, subfamily V, member 3	Luzp1	12.355	0.04913	ENSRNOG00000022402	Transcription factor
Sulfotransferase family 1A member 1	Trpv3	12.111	3.32E-07	ENSRNOG00000019606	Ion channel
Mucin 6	Sult1a1	11.715	0.03341	ENSRNOG00000019342	Neurotransmission
Potassium voltage-gated channel subfamily J member 9	Muc6	11.632	0.0074	ENSRNOG00000056817	Adhesion
Single-minded family bHLH transcription factor 2	Kcnj9	11.274	0.0008	ENSRNOG00000007645	Ion channel
	Sim2	11.092	0.0001	ENSRNOG00000054203	Transcription factor

FDR: false discovery rate.

displays a single statistically significant KEGG pathway of Calcium signaling (KEGG:04020). When drug is present (CCI CXB-NE vs. naïve) between the 584 differentially expressed genes (raw P value ≤ 0.05), cell cycle (KEGG:04110) show KEGG pathway expression; however, no significant KEGG signaling pathways between CCI DF-NE and naïve conditions are noted. Reactome pathway (www.reactome.org) analysis³³ shows that

when COX-2 is inhibited in macrophages, there is a statistically significant activation of two pertinent Reactome pathways: neutrophil degranulation (R-RNO-6798695) and the innate immune system (R-RNO-168249). Furthermore, PML-RAR alpha-regulated adapter molecule 1, Pram1, is known to be involved in neutrophil degranulation and has a fold change of 8.73 in the COX-2 inhibiting CXB-NE pain-relieved

Table 4. Top downregulated protein-coding genes differentially expressed between CCI DF-NE and CCI CXB-NE rats with an adjusted P value (FDR) \leq 0.05.

Gene description	Gene ID	Fold change	FDR	ENSEMBL gene ID	Molecular function
Histone H4 variant H4-v.11	Hist1h2ao	0.0308	0.04061	ENSRNOG00000058444	Nucleosome formation
U2 small nuclear RNA auxiliary factor 1	U2af1	0.0742	0.0218	ENSRNOG00000045860	Splicing factor
Poly (ADP-ribose) polymerase 2	Parp2	0.3284	2.58E-19	ENSRNOG00000008892	ADP-ribosylation
RNA polymerase II subunit B	Polr2b	0.3573	1.55E-05	ENSRNOG00000024779	RNA Polymerase
Bestrophin 1	Best1	0.5881	5.09E-05	ENSRNOG00000020346	Ion channel
Coiled-coil domain containing 152	Ccdc152	0.5883	0.01017	ENSRNOG00000039473	Unknown
ER membrane protein complex subunit 9	Emc9	0.6310	0.01652	ENSRNOG00000019162	Unknown
Strawberry notch homolog 2	Sbno2	0.7007	0.00027	ENSRNOG00000013987	Transcription factor
TLC domain containing 1	Tlcd1	0.7033	1.40E-08	ENSRNOG00000012579	Membrane assembly

FDR: false discovery rate.

Table 5. Differentially expressed annotated lncRNAs between CCI DF-NE and CCI CXB-NE rats with an adjusted P value (FDR) \leq 0.05.

Gene name	Fold change	FDR	ENSEMBL gene ID
AABR07033570.1	50.95	.0001	ENSRNOG00000056730
AABR07033249.1	27.06	0.049	ENSRNOG00000055160
AABR07062800.1	15.77	0.0046	ENSRNOG00000054861
Rn60_1_2212.2	4.97	4.15E-12	ENSRNOG00000062127

FDR: false discovery rate.

state. Expression changes in Importin 7 (Ipo7) and Strawberry Notch Homology 2 (Sbno2) are two genes involved in the activation of the innate immune system. Sbno2 is reduced in expression when CXB-NE is present (fold change 0.70) and Ipo7 is increased (6.9 fold change).

Genes previously implicated in neuroinflammation

Several genes that have been previously reported to exhibit differential expression in neuroinflammation and/or the neuropathic pain were independently revealed in our analysis as summarized in Tables 7 and 8. Table 7 illustrates mechanism-specific genes expressed in the pain state compared to pain relief after injection of COX-2 inhibiting CXB-NE, with up-regulation and down-regulation noted with arrow symbols. Table 8 shows previously identified cell-specific expression with specific changes following CXB-NE. Based on GO analysis using the Gene Expression Database,³⁴ genes with overlapping expression in the pain and immune responses include the purinergic ligand-gated calcium channel P2rx4, the G-protein-coupled PGE₂ receptor, Ptger1, and IL-16, a pro-inflammatory cytokine that is chemotactic for CD4+ T-lymphocytes. Genes that normally exhibit neuronal expression and that are involved with the overall

neuroinflammatory response include the sodium channels Scn8a/Nav1.6 and Scn11a/Nav1.9; the calcium channels Trpv1, Trpv3; and the NMDA receptor Grin3b/NMDAR3b. Significant expression changes occur when CXB is administered in the pain-state and include mRNAs associated with axonal growth cone (Flrt3), growth cone (LRRTM1), axon guidance (Flrt3), regulation of axon guidance (Mycbp2), response to axon injury (Flrt3), and axonogenesis (Map1a, Dst). Molecular expressions of genes involved in the immune response are noted including the β -arrestin 2 (Arrb2). Transforming growth factor β receptor signaling pathway activation including importin 7 (Ipo7) involved with the innate immune response, strawberry notch 2 (Sbno2) involved with macrophage activation, and PML-RAR alpha-regulated adaptor molecule 1 (Pram1) a component of integrin-mediated signaling as well as T cell receptor signaling, regulation of neutrophil degranulation, and lysine (K)-specific demethylase 5D (Kdm5d), which is involved with T cell antigen processing and presentation. SH2B adaptor protein 3 (Sh2b3) a component of the cellular response to chemokines and negative regulation of chemokine-mediated signaling pathways and Fanconi anemia complementation group C (Fanc) involved in myeloid cell homeostasis. All differentially expressed gene ontologies are listed in the Supplemental Table 7.

Validation of genes by qPCR

Quantitative reverse transcription PCR was conducted on RNA purified from DRG amplified with primers for TrpV3, Scn8a, Pram1, IL-16, Ipo7, Flrt3, and Ifngr (Figure 4). All of these genes exhibited elevated RNA expression in the CCI DF-NE pain-state as compared to naïve when using RNA sequencing. All of these mRNAs when individually assessed by qPCR also exhibited elevated expression in the CCI CXB-NE pain-treated state compared to when the animals are in a pain state (CCI DF-NE). These results confirm the observation that

Table 6. Gene Ontology (GO) Panther functional pathway analysis.

Functional pathway	Genes involved
5HT2 type receptor-mediated signaling pathway (P04374)	Gna11, Slca4, Plcd3, Cacna1c, Htr2b
Angiogenesis (P00005)	Pla2g4b, Fos, Pld2, Apc, Angpt2, Sphk2, Cryab
Blood coagulation (P00011)	F2r12
Cytoskeletal regulation by Rho GTPase (P00016)	Myh6
FAS signaling pathway (P00020)	Parp2
Gonadotropin-releasing hormone receptor pathway (P06664)	Gna11, Ptger1, Fos, Cacna1c, Itpr2
Heterotrimeric G-protein signaling pathway (P00026, P00027)	Kcnj9
Huntington disease (P00029)	Rhog, Fos, Htt, Grin3b, Dync1h1, Optn, Arf6
Inflammation mediated by chemokine and cytokine signaling pathway (P00031)	Myh6, Pla2g4b, Gna11, Rhog, Myh7b, Camk2g, Adcy5, Ifngr1, Itpr2
Integrin signaling pathway (P00034)	Parva, Arhgap26, Lama5, Actn3, Col10a1, Arf6, Parva, Lama3, Col5a3
Muscarinic acetylcholine receptor 2 and 4 signaling pathway (P00043)	Kcnj9
Oxidative stress response (P00046)	Pla2g4b
Nicotinic acetylcholine receptor signaling pathway (P00044)	Myh6, Myo7b, Myo19, Myo18b, Myh7b, Chrn1, Cacna1c
TCA cycle (P00051)	Aco2
VEGF signaling pathway (P00056)	Pla2g4b
Wnt signaling pathway (P00057)	Arr3, Myh6, Gna11, Wnt4, Myh7b, Apc, Pppr2r5b, Myh6b, Cdh15, Itpr2, Arr3, Smarcd3

The number of genes within the previously annotated functional pathways with significant enrichment ($FDR \leq 0.5$). Includes genes differentially expressed between CCI DF-NE and CCI CXB-NE animals. Displays genes with an $FDR \leq 0.05$ or genes with an $FDR \leq 0.5$ and exhibits more than 4 genes per pathway.

there is a shift in expression for these transcripts when CXB-NE is present.

Discussion

RNA sequencing allows for the exploration of an aspect of the molecular and biological mechanisms underlying neuropathic pain through the analyses of transcriptome changes. Identifying gene expression changes in the pain state (CCI DF-NE) is important in defining the mechanism of neuropathic pain and the sustained chronic pain response that ensues long after injury has occurred. Up until recently, relevant gene expression studies have been limited to individual genes and subset of genes via qPCR and microarrays.^{5,15,16} Although these techniques are vital in gene expression studies, they can only be utilized to identify known RNA transcripts. RNA sequencing differs in that it allows for the identification of expressed RNAs not previously known. Thus, researchers have begun to reveal RNA transcriptome changes in the affected tissues underpinning pain in small animal models.^{7,8,21,22,24} Mounting evidence indicates that differential expression of transcripts in the DRG coding for ligand-gated ion channels, cell signaling molecules, G-protein-coupled receptors, and neuroimmune-specific precursors are all involved in the establishment of the perceived pain.^{8,22,24} We sought to further this analysis by assessing whole transcriptome changes in the DRG for animals experiencing pain relief from a state of

modeled neuropathic pain as a result of treatment with the COX-2 inhibiting NSAID, CXB packaged in nanoemulsion. The effective dose of CXB is a single micro-dose, delivering COX-2 inhibiting CXB-NE to the site of injury, which provides about a week a pain relief. We reveal a novel drug effect on the differential expression of RNAs associated with neurons, activated glial cells, and multiple immune cells in the proximal dorsal root ganglion. Additionally, we use PANTHER GO and functional enrichment analyses to reveal 14 distinct pathways implicated when CXB-NE is given to CCI animals. REACTOME pathway analysis indicates an altered neuroinflammatory response with changes in neutrophil granulation and the innate immune system within the cell bodies of injured rats. Moreover, we use qPCR to explore a subset of genes that show elevated expression in CCI rats experiencing a state of pain-relief following administration with CXB-NE, compared to those in a pain state (DF-NE). This subset of genes has been previously reported in the literature to be involved in neuroinflammation.^{4,15,22,23,36,37} RNAs revealed in this current study are inclusive of both protein-coding (mRNAs) and nonprotein-coding including recently annotated lncRNAs. Overall, the impact of a precise drug inhibition of COX-2 and the corresponding reduction in PGE₂ production at the site of injury broadly influence RNA expression in multiple cell types of the corresponding DRG.

Table 7. Comparing CXB-NE (inhibiting COX-2) to DF-NE DRG reveals differentially expressed RNAs involved in underlying neuroinflammatory pain mechanisms categorized using molecular functions.

	Ion channels	Signal transduction	Synaptic transmission	Cell adhesion and migration	Neurotrophins/ Growth factors	Inflammatory signaling/ Inflammation	Eicosanoid metabolism	Transcription factors	Other
Pain response	↑Na _v 1.6 ↑Na _v 1.9 ↑Ca _v 1c ↑Ca _v 1d ↑Kcnj9 ↑Trpv1 ↑Trpv3 ↑Ncald	↑P2rx4 ↑Arrb2 ↑Mycbp2	↑Grin3b	None	↓Ntrk1	↑Ifngr1 ↑IL-16 ↑Tnfrap812	↑Ptger1 ↑Pla2g4b ↓Ptgds	None	None
Nerve regeneration		↑Gpr22 ↑Arhgap26 ↑Pice1 ↑Arhgef11 ↑Itpkc ↑Nkiras1 ↑Mycbp2	↑LRRTM1 ↑LRRTM2 ↑LRRTM3 ↓Cotl1	↑Dst ↑Frt3 ↑Lrp2bp ↑Parva	↓Ntrk1 ↑Gdf11 ↓Ltbp4 ↑Psap11	↑Map1a ↑Fkbp3	↑Pla2g4b ↓Cotl1	↓c-Fos	None
Immune response	↑Trpv1 ↑Trpv3	↑P2rx4 ↑Nkiras1 ↑Arrb2 ↑Gpr17	↑Epb4113	↑Elmo3 ↓Card14 ↑Tcalm	None	↑Ipo7 ↑Pram1 ↑Fance ↑Irgq ↑F2rl2 ↑Sh2b3 ↑Scube3 ↓Sbno2 ↑Ilf3 ↑Ifit1 ↑IL-12rb2 ↑IL-12 ↑IL-16 ↑C8a ↑Ahsa2 ↑AC127605 ↓Ctsa	↑Pla2g4b ↑Ptger1 ↓Ptgds	None	↓Nbeal2

(continued)

Table 7. Continued

	Ion channels	Signal transduction	Synaptic transmission	Cell adhesion and migration	Neurotrophins/ Growth factors	Inflammatory signaling/ Inflammation	Eicosanoid metabolism	Transcription factors	Other
Cytokine production	↑Itpr2	↑Sema4c	None	None	None	↑Angptl ↑IL-12 ↑IL-12rb2 ↑IL-16 ↑Ilf3 ↑F2rl2 ↑Hmox2	↓Ptgds	None	None
Unknown role in CCI	↓Best1	↑Atxn10 ↑Htt ↑Timp4	None	↑Acan ↑Agr2 ↓Ltbp4	↑Vasnl ↑Psap1l	None	None	None	↑Optnl ↓Fxn ↑Apob

Note: Increased and decreased expression is noted with arrow symbols ↑ and ↓. CCI: chronic constriction injury.

Table 8. Cell-specific expression of differentially expressed genes* after administration of CXB-NE.

	Ion channels	Signal transduction	Synaptic transmission	Cell adhesion and migration	Neurotrophins/ Growth factors	Inflammatory signaling/ Inflammation	Eicosanoid metabolism	Transcription factors
Neuronal	↑Na _v 1.6 ↑Na _v 1.9 ↑Scn3b ↑Cacna1c ↑Cacna1d ↑Kcnj9 ↑Kcnmb1 ↑Kcnt1 ↑Kcne3 ↑Kcnab1 ↑Trpv1 ↑Trpv3 ↑Ncald ↑Clcn7	↑P2rx4 ↑Arrb2 ↑Mycbp2 ↑Camk2g	↑Grin3b ↑Srx18 ↑Syt5 ↑LRRTM1 ↑LRRTM2 ↑LRRTM3	↑Flrt3 ↑Dst	↓Ntrk1	↑Map1a	↑Pla2g4b	None

(continued)

Table 8. Continued

	Ion channels	Signal transduction	Synaptic transmission	Cell adhesion and migration	Neurotrophins/ Growth factors	Inflammatory signaling/ Inflammation	Eicosanoid metabolism	Transcription factors
Glial cells	None	↑Arr3	None	↑Omg ↑Syne2	None	None	None	None
Macrophages	↑Trpv1 ↑Scld2a2 ↑Scld2a8 ↑Scld26a ↑Scld51a ↑Scld7a4 ↑Scld6a4 ↑Scld10a ↑Scld9a8	↑Wnt4		↑Myo7b ↑Myo9b ↑Myo19 ↑Thbs3 ↑Adgrg6 ↑Adgrg5 ↑Sphk2 ↑Muc6 ↑Muc15 ↑Elmo3 ↑Itgb1bp1 ↑Thbs3	None	↑Ifngr1 ↑Fanc ↑Fanca ↑C8a ↑Card14 ↑Ilf3 ↑Ifit1 ↑IL-12rb2 ↑IL-12 ↑IL-16 ↑IL-12rb2 ↑IL-16	↑Pla2g4b ↑Pger1 ↓Prgds	↓c-fos ↑Jmjd1c ↓Jmjd8 ↑Ncor1 ↑Ncoa2 ↑Nr2c2
Circulating monocytes	None	None	None	↑Myo7b ↑Myo19 ↑Myh6 Myh10 ↓Myh12b ↑Myh7b ↑Itgb1bp1 ↑Thbs3	None	↑Unc13d ↑Pram1	↑Pla2g4b	None
Neutrophils	None	↑Abr	None	↑Myo7b ↑Myo19 ↑Myh6 Myh10 ↓Myh12b ↑Myh7b ↑Itgb1bp1 ↑Thbs3	None	↑Pram1 ↑Ipo7 ↑F2rl2	None	None
Mast cells	None	↑Pld2	None	↑Snx17 ↑Sphk2 ↑Thbs3	None	None	↑Pla2g4b	None
T cells	None	None	None	↑Muc6 ↑Muc15 ↑Tcaim	None	↑Il12rb2 ↑IL-12 ↑IL-16	None	↓c-Fos
Endothelial cells	↑Itp2	↑Gn11 ↑Adcy5 ↑Pld2 ↑Angpt2 ↑Sphk2	None	None	None	↓Cryab	↑Pla2g4b	None

Note: Increased and decreased expression is noted with arrow symbols ↑ and ↓.
*Genes with a statistically significant raw P value or FDR value ≤0.05 are included.

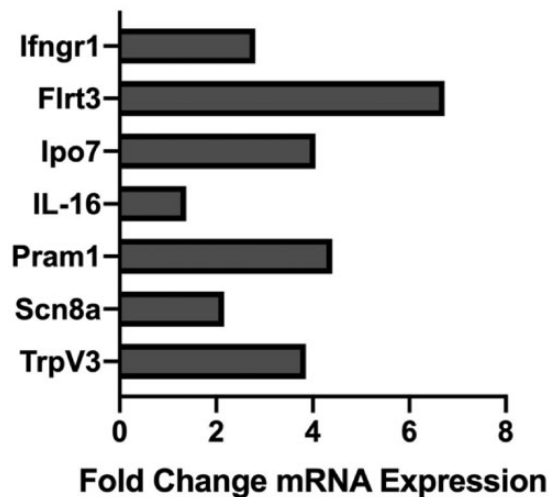


Figure 4. Individual qPCR analysis of distinct genes showing differentially expressed in the pain (CCI DF-NE) compared to the pain-relieved (CCI CXB-NE) state. CCI animals given CXB-NE exhibit increased expression of seven known neuroinflammatory genes consistent with the RNAseq analysis.

The main achievement of this study is the demonstration that treatment of neuropathic pain achieved by targeted inhibition of COX-2 in macrophages leads to changes in gene expression profiles throughout the affected peripheral nervous system; not just confined to the site of injury¹⁵ or within infiltrating macrophages. For context, previous studies using systemically, intrathecally, or subcutaneously delivered CXB demonstrated a decrease in PGE₂ and moderate attenuation of allodynia in CCI animals,^{38,39} whereas upon intraneural injection hypersensitivity persisted as well as PGE₂ levels.⁴⁰ Our studies use a theranostic nanoemulsion, which an anti-inflammatory NSAID component (CXB) utilized for treatment and a near infrared fluorescent dye to localize the nanoemulsion *in vivo*.^{5,14,15} Nanoemulsion is readily cleared from the bloodstream and introduced to the DRG by infiltrating macrophages.^{14,28,29,41} We hypothesize that the observed gene expression changes in the DRG is due to targeted COX-2 in infiltrating macrophages upon phagocytosis of the nanoemulsion from the bloodstream.^{5,14,15} In accord with previous studies, a single dose (~0.24 mg/kg) of CXB-NE one week after CCI surgery leads to a change in the number of infiltrating macrophages, revealing on day 12 while the DRG has infiltrated macrophages, the density is 40% of what is seen in the injured sciatic nerve.⁵ Also, while 63% of the macrophages in the sciatic nerve have nanoemulsion, only 19% of the macrophages in the DRG carry nanoemulsion.⁵ From a behavioral standpoint, in CCI CXB-NE animals, there is a reduction in hypersensitivity within a day of intravenous injection and a near reversal in hypersensitivity by day 12,

at which time tissue collection occurred.^{5,14,15} Furthermore, our group⁵ have shown that peak pain-relief occurs on the third and fourth day after CXB-NE treatment and persists up to six days after administration. Although gene expression changes were examined on day 12, it is likely that different subset of genes will be expressed beyond this time point. Saleem et al.⁵ also demonstrated shifts from M1 to M2 phenotypes within the injured nerve when CXB-NE is administered compared to CCI animals receiving DF-NE, revealing an increase in the number of M1 macrophages in CCI DF-NE animals on day 12.⁵ Alternatively, the number of M2 macrophages is significantly increased in injured animals receiving CXB-NE on day 12, with a parallel production on day 18 in both pain-treated and untreated pain states.⁵ At day 12, there are nearly twice as many infiltrating macrophages in the injured sciatic nerve than the corresponding DRG; interestingly, about 60% of the sciatic nerve macrophages have nanoemulsion, whereas in the DRG only about 20% carry nanoemulsion.⁵ When CXB is present, the number of macrophages at day 12 in the sciatic nerve is nearly halved but is unchanged in the DRG.⁵ By day 18, the number of macrophages in the DRG increases about three-fold, while it remains unchanged in the injured nerve.⁵ Given that analgesia persists until around day 15, this may indicate the induction and persistence of gene expression that influences the milieu of cells at the DRG long term.

Clearly, transcriptional changes are not restricted to changes in expression of genes associated with the production of PGE₂ in macrophages, instead transcriptional changes are evident for other neuroinflammation-associated genes and genes expressed in other cell types. The 25 genes with the greatest increase in expression are protein-coding genes associated with CCI CXB-NE pain relief (compared to CCI DF-NE) are illustrated in Table 4; however, the biggest differences may not be the most important in terms of underlying biology. Tables 7 and 8 refer to genes previously implicated in neuropathic pain and neuroinflammation, which display varying degrees of altered expression in this study. Genes known to be involved in neuroinflammation and found to be responsive to drug therapy in this study are listed in Tables 7 and 8. Among the differentially expressed RNAs, Phospholipase A2 Pla2g4b (involved in the hydrolysis of phospholipids in the membrane), G-protein-coupled Prostaglandin E receptor type 1 Ptger1, and Prostaglandin D2 Synthase Ptgds are involved in the production of PGE₂ after breakdown of the cell membrane. We also find the differences in Coactosin-like (COTL1), which binds to F-actin and interacts with 5-lipoxygenase in leukotriene biosynthesis. All of these are associated with the metabolism of arachidonic acid and eicosanoids, which are associated with COX-2

inhibition; and they show differential expression when CXB-NE is present in CCI animals.

We also know that on day 12, day of tissue collection, CCI animals are known to be undergoing peripheral nerve regeneration.^{5,42} Our data show that genes involved in this process are affected when drug-loaded nanoemulsion is applied to the pain state, possibly leading to an increase in factors contributing to nerve regeneration. Fibronectin leucine-rich transmembrane protein 3 Flrt3, and leucine-rich repeat transmembrane neuronal proteins LRRTM1, LRRTM2, and LRRTM3 are all differentially expressed and are known to be involved in axon outgrowth and synapse formation.⁴³

One way to think of these observations is in terms of a potential shift in cell fate, which may be occurring among several cell types during the chronic inflammatory state. The transition to chronic pain relies on significant changes in gene expression. Similarly, when COX-2 is inhibited in macrophages during the neuroinflammatory response, the shifts in RNA expression can represent realignment of cellular function representing pain-relief and possibly shifts in cell fate as was seen in the macrophage transition from M1 to M2 in the sciatic nerve in response to CXB-NE.⁵ Transcriptional and protein changes are noted in both the damaged sciatic nerve and the DRG.^{5,15,20,44} We have previously shown that intravenous injection of CXB-NE one-week postinjury results in differences in macrophage expression at the injured sciatic nerve and in the lumbar DRGs⁵ as well differential expression of a subset of mRNAs in the sciatic nerve compared to the DRGs.¹⁵ Here, we show when COX-2 is inhibited, there is an increased expression in inflammatory molecules (pro-inflammatory cytokines IL-12, Il12rb2, IL-16) and other RNAs known to be involved with cells associated with the neuroinflammatory response including Unc13d involved in intracellular trafficking and exocytosis, also Pram1 an adaptor protein involved with T-cell receptor-mediated signaling, Sh2b3 an adaptor protein involved with regulating signaling pathways and Ipo7 a nuclear transport protein. In addition, there is a down-regulation in ion channels in CCI DF-NE (Scn8a, Scn11a, Scn3b, Clcn7, Kcnj9, Kcnt1, Kcnmb1, Kcne3, Kcnh6, Kcnab1, Trpv1, Trpv3, Cacna1c, and Cacna1d) ranging from a fold change of 2.5 to 20.7, when the raw P value is ≤ 0.05 . Given these changes, it appears that select RNAs associated with neuronal expression in the DRG shift from a normal sensory neuron to a hypersensitive pain-responding neuron after CCI. Even after a pain-relieving behavioral change is evident after CXB-NE is given, RNAs typically associated with inflammation continue to exhibit increased expression on day 12. In comparison, to the injured sciatic nerve, when given CXB-NE, neuroinflammatory-associated RNAs show down-regulation, with a decreased expression of Scn9a

and TrpV3 and an increase expression in Cacna1b.¹⁵ Interestingly, a comparable RNA sequencing studying examining sex differences at the DRG after CCI revealed a modest up-regulation of Scn9a.²² It is important to note that gene expression differences exist in the DRG and sciatic nerve after CCI. We have shown previously that IL-6, IL-1 β , Scn9a/Nav1.7, Grin2b/NMDAR2b, Itgam/Cd11b, Moab, Tac1, and Trpv3 are all down-regulated in the injured sciatic nerve after CXB-NE administration, whereas Cacna1b is up-regulated.¹⁵ Similarly, some genes and their homologs exhibit differential expression in the DRG under nanoemulsion treatment. For example, in the DRG, there is an increased expression of the Calcium channel Cacna1b and sodium voltage-gated channels Nav1.6 and Nav1.8 after treatment with CXB-NE. A recent study in mice explored how DRG macrophage activation may influence sensory neurons and found a significant up-regulation of IL-1 β only in CD11b macrophages, with no evidence of IL-1 β expression in satellite cells or sensory neurons.⁴⁴ In addition, there is a shift in RNA expression typically associated with Schwann cells, macrophages, and mast cells in their inflammatory functions. RNA expression changes in cell adhesion molecules (Flrt3, Elmo3, Card14, Dst, Parva, Myo7b, Myo19, Itgb1bp1, Thsb3) is also seen, suggesting the extracellular milieu for the cells in the DRG, including the primary sensory neurons, is changing. An increase in expression of Flrt3 in the DRG has been noted in previous RNA sequencing studies.²² Furthermore, Mast cells may be in a degranulating state in the pain-relieved state, as indicated by an increase in Pram1 and Unc13d expression. We have previously shown a decrease in Mcpt1 mast cell degranulation at the site of injury when COX2 is inhibited by nanoemulsion CXB-NE.^{5,15}

This study shows decreased expression of TrpV3 RNA in the DRG while in the pain state (DF-NE) as compared to animals with COX2 inhibited by CXB-NE that are experiencing pain relief. Interestingly, we have previously shown the opposite effect in the sciatic nerve where a significant decrease in TrpV3 gene expression is evident in CCI CXB-NE animals.¹⁵ One interpretation is that TrpV3 expression at the injured sciatic nerve is prominent due to its activation by arachidonic acid metabolites in inflammatory conditions. A 2006 study by Zhu et al.⁴⁵ shows that TrpV3 is potentiated by unsaturated fatty acids such as the activation of arachidonic acid, which is targeted specifically by CXB. Furthermore, a study by Freichel et al.⁴⁶ demonstrated that activated mast cells exhibit increased expression of Trp proteins, associated with pain and degranulation.

Neuro-immune cross-talk may be associated with the increased expression of F2rl2 a 7-Transmembrane G-Protein-coupled receptor, Pram1, which is associated with T-cell receptor-mediated signaling, and Ipo7 a

nuclear transport protein. These observations are consistent with the REACTOME analysis, displaying activation of neutrophil degranulation (R-RNO-6798695) and activation of innate immune system (R-RNO-268249) pathways. Neuroimmune signaling further mediated by the purinergic receptor P2rx4 (expressed by neurons and immune cells) may lead to the increase in neutrophil and M1 macrophage infiltration after nerve injury as seen when given a systemic COX-2 inhibitor.⁴⁷ Although we have previously reported *in vitro* and *in vivo* specificity of the nanoemulsion to monocytes,⁴¹ activation of the innate immune system may lead to an increased neutrophil response after CCI. Within injured sciatic nerve tissues, we have previously identified pain and CXB-NE pain-relief shifts in M1 and M2 macrophage phenotype and mast cell degranulation activity using the same experimental conditions at day 12.⁵ Considering all of the RNA expression data from both the injured sciatic nerve¹⁵ and associated DRG cell bodies reported here, we observe that due to the CCI damage of the associated axons and surrounding cells in the sciatic nerve, RNA expression changes are apparent at not only the injured sciatic nerve^{5,14,15} but also in the cells of the DRG.

In addition to differential expression of protein-coding RNAs expressed in the DRG, noncoding RNA expression changes were investigated. The role of noncoding RNAs remains an important aspect of pain research as these RNAs actively participate in processes that coordinate gene expression.⁴⁸ One class of noncoding RNAs are lncRNAs, which are greater than 200 nucleotides in length, highly abundant and multifunctional. lncRNAs have the capacity to regulate gene expression.⁴⁹ Interestingly, we have identified four lncRNAs that are differentially expressed when CXB-NE is administered (Table 5). Each of these lncRNAs exhibit significant expression changes ranging from a nearly 5-fold increase to a 50-fold increase in CCI-CXB-NE (Table 5) and have only been recently annotated in ENSEMBL.

In summary, peripheral nerve injury resulting in behavioral hypersensitivity causes changes in RNA expression at the site of injury,¹⁵ as well as differential RNA expression evident in the corresponding cell bodies of the DRG. We also demonstrate that introducing CXB-NE not only reduces hypersensitivity^{5,14,15} but also reduces inflammation at the site of injury,^{5,14,15} the drug therapy is associated with widespread changes in the transcriptome of various cell types at the site of injury and the cells of the corresponding DRG. Even though CXB specifically attenuates COX-2 activity in the associated macrophages, the influence extends far beyond.

Acknowledgements

The authors would like to express their gratitude for the University of Pittsburgh Genomics Research Core and Genomics Analysis Core in assisting with RNA sequencing.



Declaration of Conflicting Interests

The author(s) declared no potential conflicts of interest with respect to the research, authorship, and/or publication of this article.

Funding

The author(s) disclosed receipt of the following financial support for the research, authorship, and/or publication of this article: JMJ acknowledges support from NIDA award number 1R21DA039621-01. JAP also acknowledges the Hunkele Dreaded Disease Award, Samuel and Emma Winters Foundation, the Charles Henry Leach II Fund, the Commonwealth Universal Research Enhancement Award. JAP and JMJ acknowledge support from the Duquesne University Inaugural Provost's Interdisciplinary Research Consortia Grant, which supports the Chronic Pain Research Consortium.

ORCID iDs

Muzamil Saleem  <https://orcid.org/0000-0001-9910-136X>
John A Pollock  <https://orcid.org/0000-0001-6602-3676>

Supplemental Material

Supplemental material for this article is available online.

References

1. Ji RR, Xu ZZ, Gao YJ. Emerging targets in neuroinflammation-driven chronic pain. *Nat Rev Drug Discov* 2014; 13: 533–548.
2. DeLeo J, Yezierski RP. The role of neuroinflammation and neuroimmune activation in persistent pain. *Pain* 2001; 90: 1–6.
3. Costigan M, Scholz J, Woolf CJ. Neuropathic pain: a maladaptive response of the nervous system to damage. *Annu Rev Neurosci* 2009; 32: 1–32.
4. Vasudeva K, Vodovotz Y, Azhar N, Barclay D, Janjic JM, Pollock JA. In vivo and systems biology studies implicate IL-18 as a central mediator in chronic pain. *J Neuroimmunol* 2015; 283: 43–49.
5. Saleem M, Deal B, Nehl E, Janjic JM, Pollock JA. Nanomedicine-driven neuropathic pain relief in a rat model is associated with macrophage polarity and mast cell activation. *Acta Neuropath Comm* 2019; 7: 108.
6. Usoskin D, Furlan A, Islam S, Abdo H, Lonnerberg P, Lou D, Hjerling-Leffler J, Haeggstrom J, Kharchenko O, Kharchenko PV, Linnarsson S, Ernfors P. Unbiases classification of sensory neuron types by large-scale single-cell RNA sequencing. *Nat Neurosci* 2015; 18: 145–156.
7. Gong L, Wu J, Zhou S, Wang Y, Qin J, Yu B, Gu X, Yao C. Global analysis of transcriptome in dorsal root ganglia

- following peripheral nerve injury in rats. *Biochem Biophys Res Commun* 2016; 478: 206–212.
8. Wu S, Lutz BM, Miao X, Liang L, Mo K, Chang Y, Du P, Soteropoulos P, Tian B, Kaufman AG, Bekker A, Hu Y, Tao Y. Dorsal root ganglion transcriptome analysis following peripheral nerve injury in mice. *Mol Pain* . 2016; 12: 1–114.
 9. Bennett GJ, Xi J. A peripheral mononeuropathy in rat that produces disorders of pain sensation like those seen in man. *Pain* 1988; 33: 87–107.
 10. Gabay E, Tal M. Pain behavior and nerve electrophysiology in the CCI model of neuropathic pain. *Pain* 2004; 110: 354–360.
 11. Jaggi AS, Jain V, Singh N. Animal models of neuropathic pain. *Fundam Clin Pharmacol* 2011; 25: 1–28.
 12. Challa SR. Surgical animal models of neuropathic pain: pros and cons. *Int J Neurosci* 2015; 125: 170–174.
 13. Austin PJ, Wu A, Moalem-Taylor G. Chronic constriction of the sciatic nerve and pain hypersensitivity in rats. *J Vis Exp* 2012; 61: e3393.
 14. Janjic JM, Vasudeva K, Saleem M, Stevens A, Liu L, Patel S, Pollock JA. Low-dose NSAIDs reduce pain via macrophage targeted nanoemulsion delivery to neuroinflammation of the sciatic nerve in rat. *J Neuroimmunol* 2018; 318: 72–79.
 15. Stevens AM, Liu L, Bertovich D, Janjic JM, Pollock JA. Differential expression of neuroinflammatory mRNAs in the rat sciatic nerve following chronic constriction injury and pain-relieving nanoemulsion NSAID delivery to infiltrating macrophages. *Int J Mol Sci* 2019; 20: 5269.
 16. LaCroix-Fralish ML, Austin J, Zheng FY, Levitin DJ, Mogil JS. Patterns of pain: meta-analysis of microarray studies of pain. *Pain* 2011; 152: 1888–1898.
 17. Dib-Hajj SD, Fjell J, Cummins TR, Zheng Z, Fried K, LaMotte R, Black JA, Waxman SG. Plasticity of sodium channel expression in DRG neurons in the chronic constriction injury of neuropathic pain. *Pain* 1999; 83: 591–600.
 18. Obata K, Yamanaka H, Fukuoka T, Yi D, Tokunaga A, Hashimoto N, Yoshikawa H, Noguchi K. Contribution of injured and uninjured dorsal root ganglion neurons to pain behavior and the changes in gene expression following chronic constriction injury of the sciatic nerve in rats. *Pain* 2003; 101: 65–77.
 19. Parkitna JR, Korostynski M, Kaminska-Chowaniec D, Obara I, Mika J, Przewlocka B, Przewlocki R. Comparison of gene expression profiles in neuropathic and inflammatory pain. *J Phys Pharm* 2006; 57: 401–414.
 20. Vasudeva K, Andersen K, Zeyzus-Johns B, Hitchens TK, Patel SK, Balducci A, Janjic JM, Pollock JA. Imaging neuroinflammation *in vivo* in a neuropathic pain rat model with near-infrared fluorescence and ¹⁹F magnetic resonance. *PLoS One* 2014; 9: e90589.
 21. Yin C, Hu Q, Liu B, Tai Y, Zheng X, Li Y, Xiang X, Wang P, Liu B. Transcriptome profiling of dorsal root ganglia in a rat model of complex regional pain syndrome type-I reveals potential mechanisms involved in pain. *J Pain Res* 2019; 12: 1201–1216.
 22. Stephens K E, Zhou W, Ji Z, Chen Z, He S, Ji H, Guan Y, Taverna SD. Sex differences in gene regulation in the dorsal root ganglion after nerve injury. *BMC Genomics* 2019; 20: 147.
 23. Ray P, Torck A, Quigley L, Wangzhou A, Neiman M, Rao C, Lam T, Kim J, Kim TH, Zhang MQ, Dussor G, Price TJ. Comparative transcriptome profiling of the human and mouse dorsal root ganglia: an RNA-seq-based resource for pain and sensory neuroscience research. *Pain* 2018; 159: 1325–1345.
 24. Uttam S, Wong C, Amorim IS, Jafarnejad SM, Tansley SN, Yang J, Prager-Khoutorsky M, Mogil JS, Gkogkas C G, Khoutorsky A. Translational profiling of dorsal root ganglia and spinal cord in a mouse model of neuropathic pain. *Neurobiol Pain* 2018; 4: 35–44.
 25. Liu L, Karagoz H, Herneisey M, Zor F, Komatsu T, Loftus S, Janjic BM, Gorantla VS, Janjic JM. Sex differences revealed in a mouse CFA inflammation model with macrophage targeted nanotheranostics. *Theranostics* 2020; 10: 1694–1707.
 26. Dixon WJ. The up-and-down method for small samples. *J Am Stat Assn* 1965; 60: 967–978.
 27. Patel SK, Janjic JM. Macrophage targeted theranostics as personalized nanomedicine strategies for inflammatory disease. *Theranostics* 2015; 5: 150–172.
 28. Saleem M, Stevens AM, Deal B, Liu L, Janjic JM, Pollock JA. A new best practice for validating tail vein injections in rat with near-infrared-labeled agents. *JoVE* 2019; 146: e59295.
 29. Patel SK, Patrick MJ, Pollock JA, Janjic JM. Two-color fluorescent (near-infrared and visible) triphasic perfluorocarbon nanoemulsions. *J Biomed Opt* 2013; 18: 101312.
 30. Mueller O, Lightfoot S, Schroeder A. RNA integrity number (RIN)-standardization of RNA quality control. *Agilent Technol* 2016; publication PN 5989-1165EN.
 31. Mi H, Muruganujan A, Huang X, Ebert D, Mills C, Guo X, Thomas PD. Protocol update for large-scale genome and gene function analysis with the PANTHER classification system (v.14.0). *Nat Protoc* 2019; 14: 703–721.
 32. Uku R, Kolberg L, Kuzmin I, Arak T, Adler P, Peterson H, Vilo J. g:Profiler: a web server for functional enrichment analysis and conversion of gene lists (2019 update). *Nucleic Acids Res* 2019; 47: W191–W198.
 33. Croft D, Mundo AF, Haw R, Milacic M, Weiser J, Wu G, Caudy M, Garapati P, Gillespie M, Kamdar MR, Jassal B, Jupe S, Matthews L, May B, Palatnik S, Rothfels K, Shamovsky V, Song H, Williams M, Birney E, Hermjakob H, Stein L, D'Eustachio P. The Reactome pathway knowledgebase. *Nucleic Acids Res* 2014; 42: D472–D477.
 34. Ashburner M, Ball CA, Blake JA, Botstein D, Butler H, Cherry JM, Davis AP, Dolinski K, Dwight SS, Eppig JT, Harris MA, Hill DP, Issel-Tarver L, Kasarskis A, Lewis S, Matese JC, Richardson JE, Ringwald M, Rubin GM, Sherlock G. Gene ontology: tool for the unification of biology. The Gene Ontology Consortium. *Nat Genet* 2019; 2: 25–29.
 35. Livak KJ, Schmittgen TD. Analysis of relative gene expression data using real-time quantitative PCR and the 2^{-ΔΔCT} method. *Methods* 2001; 25: 402–408.

36. Ma W and Quirion R. Does COX2-dependent PGE₂ play a role in neuropathic pain?. *Neuroscience Letters*. 2008; 437: 165–169. 10.1016/j.neulet.2008.02.072
37. Wang Y, Zhang X, Guo Q, Zou W, Huang C, Yan J. Cyclooxygenase inhibitors suppress the expression of P2X3 receptors in the DRG and attenuate hyperalgesia following chronic constriction injury. *Neurosci Lett* 2010; 478: 77–81.
38. Syriatowicz JP, Hu D, Walker JS, Tracey DJ. Hyperalgesia due to nerve injury: role of prostaglandins. *Neuroscience* 1999; 94: 587–594.
39. Zhao Z, Chen SR, Eisenach JC, Busija DQ, Pan HL. Spinal cyclooxygenase-2 is involved in development of allodynia after nerve injury in rats. *Neuroscience* 2000; 97: 743–748.
40. Schafers M, Marziniak M, Sorkin LS, Yaksh TL, Sommer C. Cyclooxygenase inhibition in nerve injury- and TNF-induced hyperalgesia in the rat. *Exp Neurol* 2004; 185: 160–168.
41. Patel S K, Beaino W, Anderson CJ, Janjic JM. Theranostic nanoemulsions for macrophage COX-2 inhibition in a murine inflammation model. *Clin Immunol* 2015; 160: 59–70.
42. Staaf S, Oerther S, Lucas G, Mattsson JP, Ernfors P. Differential regulation of TRP channels in a rat model of neuropathic pain. *Pain* 2009; 114: 187–199.
43. Sollner C, Wright GJ. A cell surface interaction network if neural leucine-rich repeat receptors. *Genome Biol* 2009; 10: R99.
44. Yu X, Liu H, Hamel KA, Morvan MG, Yu S, Leff J, Guan Z, Braz JM, Basbaum AI. Dorsal root ganglion macrophages contribute to both the initiation and persistence of neuropathic pain. *Nat Commun* 2020; 11: 264.
45. Hu H, Xiao R, Wang C, Gao N, Colton CK, Wood JD, Zhu MX. Potentiation of TRPV3 channel function by unsaturated fatty acids. *J Cell Physiol* 2006; 208: 201–212.
46. Freichel M, Almering J, Tsvilovskyy V. The role of TRP proteins in mast cells. *Front Immunol* 2012; 3: 1–15.
47. de Rivero Vaccari JP, Bastien D, Yurcisin G, Pineau I, Dietrich W D, De Koninck Y, Keane R W, Lacroix S. P2X4 receptors influence inflammasome activation after spinal cord injury. *J Neurosci* . 2012; 32: 3058–3066.
48. Zhou J, Xiong Q, Chen H, Yan C, Fan Y. Identification of the spinal expression profile of non-coding RNAs involved in neuropathic pain following spared nerve injury by sequence analysis. *Front Mol Neurosci* 2017; 10: 1–22.
49. Wu S, Bono J, Tao Y. Long noncoding RNA: a potential target for neuropathic pain. *Expert Opin Ther Targets* 2019; 23: 15–20.